Metrology of Dye-sensitized Solar Cells

Leo Furnell[a], Peter J. Holliman[a*], Rosie Anthony[a], Arthur Connell[a], Eurig W. Jones[a], Christopher P. Kershaw[a]
[a] College of Engineering, Swansea University, Swansea,
* p.j.holliman@swansea.ac.uk

Introduction

Due to growing interest in the increased levels of atmospheric CO_2 from the burning of fossil fuels, which contribute to climate change; there is a drive towards mitigating these negative effects. One mitigation method to be considered is the use of renewable energy, such as solar energy [1]. Harvesting energy from the sun *via* the development of photovoltaic (PV) technology has the potential to produce more energy for the planet than is required if harvested efficiently [2]. PV devices use the energy from the sun and convert it into electricity using photochemical reactions [2]. In 1991, O'Regan and Grätzel reported a new type of dye-sensitized solar cell (DSCs), which was a breakthrough in technology using mesoporous TiO_2 sensitized with Ru-bipyridyl dye to enhance photo-current [3]. Since this, there has been significant progress and interest in DSC devices, due to their potential to be low cost, their ease of preparation, good performance and potential to have a positive environmental impact. DSCs are an attractive source of renewable energy due to being made from earth abundant materials, low toxicity, low light operation and potential to be recycled at the end of their lifetime. However, in order to be able to compete with fossil fuels and be commercially viable, DSCs must have a scalable process and it is essential to have lifetimes of at least 20 years [4,5].

For industrial application, continuous processing is preferable, rather than batch processing and this means there needs to be a mechanism of understanding and improving the process. It is important to develop a method of obtaining feedback information in order to achieve in-line processing control, thus enabling flexibility of processing. Metrology is the scientific study of measurement and can be used to gain quantifiable information of a process *in situ* in order to enable and support production by improving quality and productivity [6]. In this paper, we propose that in-line metrology using digital imaging methods can be used as a mechanism to provide this feedback data continuously, leading to process control in an upscaling context of a production system. This feedback loop can allow the production line to work at an optimum by providing quality control and leading to the optimum yield being produced. We will use fast dyeing as an example of upscaling a process. Fast dyeing DSCs is favoured over the traditional and expensive passive dyeing process. Previous work has been carried out to optimise the fast dyeing process, providing a rapid and efficient method of sensitising DSCs [7].

It is believed that by providing a feedback loop in real time, in-line metrology will improve yield, productivity, speed of process, whilst reducing the costs [8]. An example of this, is the setting of lower and upper limits of dye loading. This monitoring of the dye uptake using process control software would allow the process to stop when a certain level is met, thus allowing homogeneous dyeing at a fraction of the cost. Dye loading is an important aspect of DSC technology as it is important to utilise as many of the dye sites as possible on the surface of the titania for maximum efficiency of the cell [9]. As such, co-sensitisation of dyes is a technique that may improve cell efficiencies by absorbing light at different wavelengths [10].

We would also like to propose the interrogation of different wavelengths of available light as a method to investigate device processing and monitoring. Imaging processes under different λ of light means that our current view of the process could be expanded and inevitably new things may be seen, allowing further control.

Experimental

Metrology of Dye Solutions

Dye solutions of N719, D131, D35, SQ1, SQ2 and methylene blue were prepared in ethanol at a concentration of 0.5mM (Figure1a). Each dye solution was split into two and added to separate sample bottles. The first bottle of each dye was left as stock solution and the second bottle had an

additive of (10mM) 2,2,6,6-tetramethyl-4-piperidinol. Solutions were then sonicated and placed on a south-westerly facing window to allow for natural light exposure. Images were taken after using a Canon EOS 1100D camera with an 18-55 VR lens at 0, 21 and 64 days.

Device Fabrication

Electrodes were constructed from TEC7 conductive glass (Pilkington) and cleaned by sonication in acetone for 15 min. Photo electrodes were constructed by doctor blading (Dyesol) Active Opaque paste onto the glass and sintered at 550°C in a Carbolite ashing furnace. Counter electrodes were constructed using (Dyesol) PT-01 platinum paste which was deposited on the surface of the glass with a pipette. The electrodes were then sintered at 450°C in a Carbolite tube furnace. The two electrodes were joined together with a 20µm Surlyn™ (DuPont) thermoplastic gasket at 150°C using a heat press. The electrolyte was then injected into the cell cavity and the cell was sealed with additional Surlyn™ and a glass microscope slide using a soldering iron.

Metrology of DSC Devices

For light soaking samples, devices were exposed simultaneously in a Photosimile 200 lightbox with a consistent light intensity of $5Wm^{-2}$ (6000lux). Images were taken using time-lapse photography every 5 seconds using a Canon EOS 1100D camera and an 18-55 VR lens. Contrast controls were also added to give 100% baselines for black and white. A clock was added to ensure images were taken on the correct timescale. A grid was used to organise samples and ensure the correct position was used for image analysis. This was essential, as a macro was used with the program (Sigma Scan Pro 5) to select the active area of each device and measure the values of red, green and blue on the RGB colour model (0-255). The macro also allowed the control area to be analysed to monitor for changes in light levels.

UV Imaging

Images were taken using a Nikon D70 with a Nikkor 50mm lens. These were selected due to the lack of UV filters in older camera equipment, as anti-reflective coatings were applied to camera lenses for general use in 1941 [11]. Images were illuminated under a Spectroline e-series UV lamp with an output wavelength of 365 nm.

Results and Discussion

Natural Light Exposure

We have investigated the colour of dye solutions during light soaking and quantified changes with RGB analysis. This established a strong correlation between dye degradation and a change in RGB values.

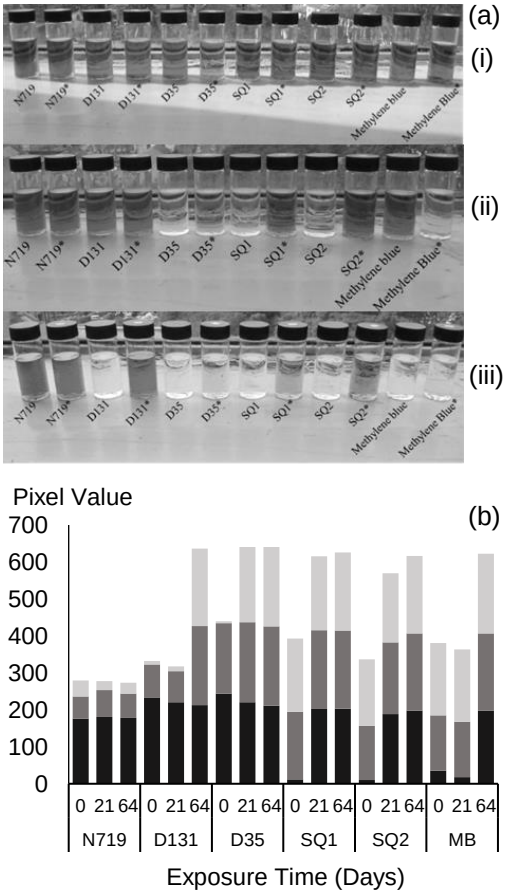

Figure 1a. Dye solutions (0.5mM) (i) before light exposure, (ii) after 20d light exposure and (iii) after 2 months exposure. Dyes marked * had an additive of 10 mmol 2,2,6,6-tetramethyl-4-piperidinol added to the solution. Images were recorded with a 28mm lens, ISO 100 and white balance of 0. Note: the samples that appear white in the image have degraded significantly and the darker solutions have not degraded.

Figure 1b. Red, green and blue (RGB) analysis of dye solutions at 0, 21 and 64 days of natural light exposure.

Figure 1a shows dye colour changes when exposed to natural light. These colour changes suggest degradation of the dye has occurred resulting in a decreased colour intensity. The images also show

differences between the rates that dyes degrade as D35 shows a significant difference between 0 and 64 days whereas N719 shows very little change.

Figure 1b shows a significant range in stabilities between dye solutions. N719 shows very little change in RGB values, indicating a high stability. D131 shows a small change initially but after 64 days all three colours are roughly equal. This indicates that the solution has turned transparent showing that the dye has significantly degraded. D35 shows equal RGB values after just 21 days indicating a high rate of degradation. SQ1 also shows a high rate of degradation with almost equal RGB values after 21 days and equal values after 64 days. SQ2 shows a slightly slower rate of degradation than SQ1. The RGB values for SQ2 are similar after 21 days indicating degradation has started to occur. After 48 days the values are roughly equal indicating significant degradation. Methylene blue dye shows some initial degradation after 21 days and a more substantial degradation after 48 days.

To investigate stability, an additive of 2,2,6,6-tetramethyl-4-piperidinol (TMP) was added each of the dye solutions. This was intended to slow degradation caused by oxygen radicals [12], since TMP is a free radical scavenger [13]. The solutions with the additive were exposed at the same time as the solutions without additive. This ensured that light exposure levels would be consistent between the two. The data from the RGB analysis is shown in Figure 2.

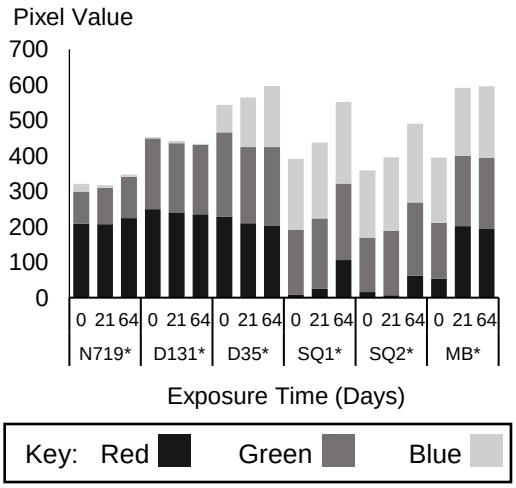

Figure 2. Red, green and blue (RGB) analysis of dye solutions with 2,2,6,6-tetramethyl-4-piperidinol at 0, 21 and 64 days of natural light exposure.

Figure 2 shows that the rate of degradation has been slowed in D131, D35, SQ1 and SQ2 dye solutions with D131 stabilised to 64 days. This is indicated by an increase in the time taken for all three values to become roughly equal. TMP had the opposite effect in N719 and methylene blue solutions and increased the rate of degradation. These data suggest that the use of TMP with these two dyes would be inadvisable in full operation. Overall, however, the majority of the dyes were stabilised by the TMP, making it a useful additive for extending dye lifetime.

Metrology of DSC Devices

Previous work by this group focused on comparing RGB analysis to IV data obtained from solar simulation. The solar simulator data is shown in Figure 3.

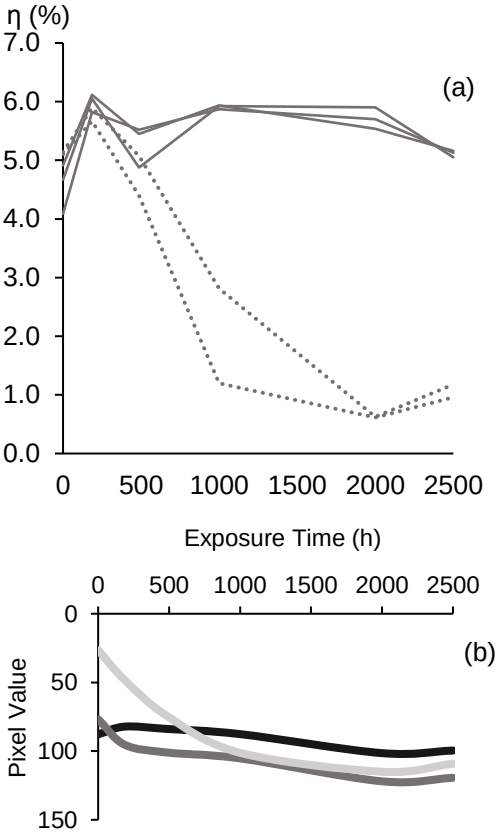

Figure 3a. Efficiency against time for selected N719 DSC devices, measured over 2500h of light soaking. **Figure 3b.** RGB analysis of the electrolyte colour in devices without a UV filter. Redrawn from work published previously by this group[4].

Figure 3a is concordant with the literature that devices made with N719 remain highly stable, with little change in efficiency over 2500 h [14]. Conversely, the devices without UV filters degrade significantly in

the first 1000 h. Figure 3b shows RGB analysis of an unfiltered cell with a gradual increase in the blue value. An increase in the blue value corresponds to a decrease in yellow colour as they opposing colours. Further analysis of device area (dyed TiO_2 vs only electrolyte) indicates bleaching of the electrolyte which is the cause of the degradation in the devices[15]. This shows a clear link between the device efficiency and colour of the electrolyte.

Wavelength Imaging

In addition to looking at the visible range of light we are also studying the UV and NIR ranges. As an example, images taken of a rose under UV light show a very different picture compared to what we see under visible light, as shown in Figure 4.

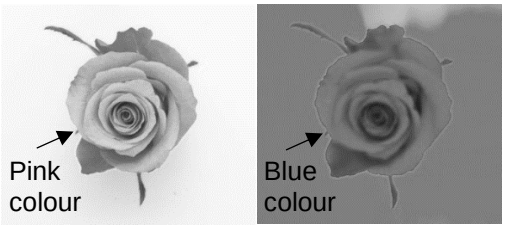

Figure 4. Image of a rose (left) under normal light and (right) under UV light.

The possibility of imaging devices in the same way has great potential. UV light may indicate features which would otherwise be invisible to the naked eye.

Conclusions

Using in-line digital imaging metrology to provide continuous data in a real-time feedback loop, is an innovative and highly useful mechanism to provide process control within a production system. We have shown that the method works well with the study of device lifetime and it is likely that this approach will prove to be a useful tool with processing. Allowing a greater level of control, during continuous processing when upscaling a process, will not only be useful but time and cost effective in an industrial context.

Acknowledgements

We gratefully acknowledge funding provided by the European Union and Welsh Government for Sparc II (LF, RA), from the Welsh Government for Sêr Cymru (PJH) and NRN (CPK) and from EPSRC EP/M015254/1 (AC, EWJ), the EPSRC UK National Mass Spectrometry Facility at Swansea University and Pilkington-NSG for TEC™ glass.

References

1. J. G. Canadell, C. Le Quéré, M. R. Raupach, C. B. Field, E. T. Buitenhuis, P. Ciais, T. J. Conway, N. P. Gillett, R. A. Houghton, G. Marland, *Proceedings of the National Academy of Sciences of the United States of America*, 2007, **104**, 18866–18870.
2. J. Wu, Z. Lan, J. Lin, M. Huang, Y. Huang, L. Fan, G. Luo, *Chemical Reviews*, 2015, **115**, 2136–2173.
3. B. O'Regan, M. Grätzel, *Nature*, 1991, **353**, 737–740.
4. L. Furnell, P. J. Holliman, A. Connell, E. W. Jones, R. J. Hobbs, C. P. Kershaw, R. Anthony, J. R. Searle, T. M. Watson, J. McGettrick, *Sustainable Energy Fuels*, 2017, DOI: 10.1039/C7SE00015D.
5. R. Harikisun, H. Desilvestro, *Solar Energy*, 2011, **85**, 1179–1188.
6. H. Kunzmann, T. Pfeifer, R. Schmitt, *CIRP Annals- Manufacturing Technology*, 2005, **54**, 155–168.
7. P. J. Holliman, M. L. Davies, A. Connell, B. Vaca Velasco, T. M. Watson, *Chemical Communications*, 2010, **46**, 7256–7258.
8. R. M. Swanson, *Prog. Photovolt: Res. Appl.*, 2006, **14**, 443–453.
9. M. Grätzel, *Inorganic Chemistry*, 2005, **44**, 6841–6851.
10. S. L. Bayliss, J. M. Cole, P. G. Waddell, S. McKechnie, X. Liu, *Journal of Physical Chemistry C*, 2014, **118**, 14082–14090.
11. B. Salt, *Film Quarterly*, 1976, **30**, 19–32.
12. I. K. Konstantinou, T. a. Albanis, *Applied Catalysis B: Environmental*, 2004, **49**, 1–14.
13. P. Pospíšil, *Biochimica et Biophysica Acta - Bioenergetics*, 2012, **1817**, 218–231.
14. N. Kato, Y. Takeda, K. Higuchi, A. Takeichi, E. Sudo, H. Tanaka, T. Motohiro, T. Sano, T. Toyoda, *Solar Energy Materials and Solar Cells*, 2009, **93**, 893–897.
15. M. Carnie, D. Bryant, T. Watson, D. Worsley, *International Journal of Photoenergy*, 2012, 524590.